

# Defective dendritic cell migration and activation of adaptive immunity in PI3K $\gamma$ -deficient mice

Annalisa Del Prete<sup>1,7</sup>, William Vermi<sup>2</sup>, Erica Dander<sup>1</sup>, Karel Otero<sup>1</sup>, Laura Barberis<sup>3</sup>, Walter Luini<sup>1</sup>, Sergio Bernasconi<sup>1</sup>, Marina Sironi<sup>1</sup>, Amerigo Santoro<sup>2</sup>, Cecilia Garlanda<sup>1</sup>, Fabio Facchetti<sup>2</sup>, Matthias P Wymann<sup>4</sup>, Annunciata Vecchi<sup>1</sup>, Emilio Hirsch<sup>3</sup>, Alberto Mantovani<sup>1,5</sup> and Silvano Sozzani<sup>1,6,\*</sup>

<sup>1</sup>Istituto Ricerche Farmacologiche 'Mario Negri', Milan, Italy,

<sup>2</sup>Department of Pathology, University of Brescia, Italy, <sup>3</sup>Department of Genetic, Biology and Biochemistry, University of Turin, Turin, Italy,

<sup>4</sup>University of Fribourg, Fribourg, Switzerland, <sup>5</sup>Centro IDET, Institute of General Pathology, University of Milan, Milan, Italy and <sup>6</sup>Section of General Pathology and Immunology, University of Brescia, Brescia, Italy

**Gene-targeted mice were used to evaluate the role of the gamma isoform of phosphoinositide 3-kinase (PI3K $\gamma$ ) in dendritic cell (DC) migration and induction of specific T-cell-mediated immune responses. DC obtained from PI3K $\gamma$ -/- mice showed a reduced ability to respond to chemokines *in vitro* and *ex vivo* and to travel to draining lymph nodes under inflammatory conditions. PI3K $\gamma$ -/- mice had a selective defect in the number of skin Langerhans cells and in lymph node CD8 $\alpha$ - DC. Furthermore, PI3K $\gamma$ -/- mice showed a defective capacity to mount contact hypersensitivity and delayed-type hypersensitivity reactions. This defect was directly related to the reduced ability of antigen-loaded DC to migrate from the periphery to draining lymph nodes. Thus, PI3K $\gamma$  plays a nonredundant role in DC trafficking and in the activation of specific immunity. Therefore, PI3K $\gamma$  may be considered a new target to control exaggerated immune reactions.**

*The EMBO Journal* advance online publication, 19 August 2004; doi:10.1038/sj.emboj.7600361

**Subject Categories:** signal transduction; immunology

**Keywords:** chemokines; chemotaxis; contact hypersensitivity; dendritic cells; PI3K $\gamma$ -/- mice

## Introduction

Dendritic cells (DC) are potent antigen-presenting cells with a unique ability in inducing T- and B-cell response as well as immune tolerance (Steinman, 1991; Banchereau *et al*, 2000; Steinman *et al*, 2003). DC reside in an immature state in peripheral tissues where they exert a sentinel function for incoming antigens (Cella *et al*, 1997; Banchereau and

Steinman, 1998). Following an encounter with antigen, in the context of an inflammatory situation, DC undergo a process of maturation, which enhances their antigen-presenting cell function and promotes their migration to the draining lymph nodes (Cyster, 1999; Sallusto and Lanzavecchia, 1999; Allavena *et al*, 2000; Banchereau *et al*, 2000). The proper localization of DC to secondary lymphoid organs and their recruitment at sites of inflammation in response to chemotactic stimuli are critical for an optimal immune response (Förster *et al*, 1999; Gunn *et al*, 1999).

Migration of leucocytes, including DC, to inflammatory sites depends on a cascade of discrete events, which are mediated in part by chemokines and their receptors (Baggiolini, 1998; Allavena *et al*, 2000; Zlotnik and Yoshie, 2000). Local production of inflammatory chemokines (e.g. CCL3, CCL5, CCL2 and CCL20) is responsible for the recruitment of immature DC, or their precursors, to sites of inflammation (Cyster, 1999; Sallusto and Lanzavecchia, 1999; Allavena *et al*, 2000; McColl, 2002). Similarly, CCL21 and CCL19 are pivotal for the migration of maturing DC to draining lymph nodes (Ngo *et al*, 1998; Sozzani *et al*, 1998; Willmann *et al*, 1998; Förster *et al*, 1999; Gunn *et al*, 1999). While it is conceivable that inflammatory chemokines are key players for leucocyte recruitment at the site of inflammation, the identity of chemokines and/or additional signals that attract DC precursors in steady-state conditions is still elusive (Cavanagh and Von Andrian, 2002). DC are heterogeneous, and different DC subsets express different but overlapping patterns of chemokine receptors (Penna *et al*, 2001). Langerhans cells (LC) are characterized by the expression of CCR6, and the production of CCL20, the CCR6 ligand, induces LC accumulation in pathological conditions (Charbonnier *et al*, 1999; Homey *et al*, 2000). Myeloid CD11c<sup>+</sup> blood DC respond to a wide array of inflammatory chemokines and classical chemotactic agonists, whereas circulating CD123<sup>+</sup> plasmacytoid DC express only CXCR4 as a functional chemotactic receptor (Penna *et al*, 2001). The different repertoire of chemokine receptors is likely to be responsible for the different distribution of DC subsets at sites of inflammation and immune response.

Recent work has outlined the importance of lipid products derived from phosphoinositide 3-kinases (PI3K) in leucocyte polarization and migration (Rickert *et al*, 2000). The PI3K family is divided into three main groups of enzymes (class I, II and III) on the basis of the phosphoinositides that they preferentially utilize as substrates (Wymann *et al*, 2000; Sasaki *et al*, 2002). Attention has recently been focused on the members of class I PI3Ks, since these enzymes were found to be the isoforms that are activated upon receptor stimulation (Sasaki *et al*, 2002; Ward, 2004). While the  $\alpha$ ,  $\beta$  and  $\delta$  isoforms (class IA) are activated by tyrosine kinases, the  $\gamma$  isoform (class IB) is activated by the  $\beta\gamma$  component of heterotrimeric G proteins (Wymann *et al*, 2000; Sasaki *et al*, 2002; Brock *et al*, 2003). Accordingly, PI3K $\gamma$  is associated with seven-transmembrane spanning receptors including

\*Corresponding author. Section of General Pathology and Immunology, University of Brescia, viale Europa 11, 25123 Brescia, Italy.

Tel.: +39 030 371 7282; Fax: +39 030 370 1157;

E-mail: sozzani@med.unibs.it

<sup>7</sup>Present address: Section of Medical Biochemistry, University of Bari, Bari, Italy

Received: 12 March 2004; accepted: 16 July 2004

chemotactic receptors (Stoyanov *et al*, 1995; Stephens *et al*, 1997; Wymann *et al*, 2000), and plays an important role in macrophage and neutrophil recruitment to inflammatory sites and in mast cell function (Hirsch *et al*, 2000; Li *et al*, 2000; Sasaki *et al*, 2000; Laffargue *et al*, 2002). The aim of the present work was to characterize the role of PI3K $\gamma$  in DC recruitment *in vitro* and *in vivo*, using PI3K $\gamma$ -/- mice (Hirsch *et al*, 2000). The results presented here show that PI3K $\gamma$  plays a nonredundant role in DC migration *in vitro*, *ex vivo* and *in vivo*. Most importantly, these results show that the reduced ability of antigen-loaded DC to travel *in vivo* is responsible for the impaired ability of PI3K $\gamma$ -/- mice to mount T-cell-mediated specific immune responses in different experimental systems.

## Results

### Defective migration of PI3K $\gamma$ -/- DC

Purified CD34<sup>+</sup> cells from PI3K $\gamma$ -/- mice differentiated *in vitro* into seemingly normal DC. DC from PI3K $\gamma$ -/- mice did not express the PI3K $\gamma$  protein, as assessed by Western blot analysis, but were similar to wild-type (WT) DC in terms of membrane phenotype, dextran-fluorescein isothiocyanate (FITC) uptake, mixed leucocyte reaction (MLR) activity, expression of chemokines and chemokine receptors, and cytokine production (Figure 1A–J). However, immature DC obtained from PI3K $\gamma$ -/- mice expressed an impaired ability to migrate *in vitro* using two different chemotactic assays, namely, the ‘leading front’ assay, which evaluates the ability of migrating cells to penetrate into a nitrocellulose filter (Zigmond and Hirsch, 1973) and the ‘Transwell insert’ assay, which evaluates the number of cells that are able to go across a thin polycarbonate filter (Penna *et al*, 2001). Severe inhibition of PI3K $\gamma$ -/- DC migration was observed using both immature DC, in response to the inflammatory chemokines CCL3 and CCL5, and TNF-mature DC tested for their migration to CCL19 (Figure 2A and B). On the contrary, no difference in the migration of PI3K $\gamma$ -/- versus WT DC was observed in response to phorbol 12-myristate 13-acetate (PMA) (Figure 2B), a PI3K $\gamma$ -independent chemotactic factor (Hirsch *et al*, 2000). PI3K $\gamma$ -/- and WT DC expressed similar levels of chemokine receptors evaluated as mRNA levels (Figure 1J), FACS analysis (CCL2) and CCL3 binding sites (data not shown). Taken together, these results rule out the possibility that the impaired migration of PI3K $\gamma$ -/- DC is dependent on a reduced expression of chemokine receptors.

CD34-derived DC were then tested for their ability to migrate *in vivo*, an assay that depends on the engagement of chemotactic receptors and is *Bordetella pertussis* toxin sensitive (data not shown). Mature DC from both PI3K $\gamma$ -/- and WT mice were 5-(and 6)-carboxyfluorescein diacetate succinimidyl ester (CFSE)-labelled and injected into the footpad of WT recipient animals. Figure 2C shows that along the entire kinetics investigated (up to 72 h) a significantly ( $P < 0.05$ ) reduced number of PI3K $\gamma$ -/- DC reached popliteal draining lymph nodes compared to WT. A similar degree of inhibition was present when labelled PI3K $\gamma$ -/- DC were injected in PI3K $\gamma$ -/- mice (Figure 2D). A statistically significant inhibition was also observed when WT DC were injected in PI3K $\gamma$ -/- mice (64.2% at 48 h), compared to WT DC in WT mice. This latter result indicates that in spite of the normal architecture of the lymph nodes in PI3K $\gamma$ -/- mice

(Figure 3Aa and b), the reduced total cellularity present in PI3K $\gamma$ -/- lymph nodes (Figure 4D) plays a negative role in the homing of normal DC. Histological analysis of popliteal draining lymph nodes from PI3K $\gamma$ -/- showed that upon subcutaneous injection, CFSE-labelled DC normally localized in the paracortical T-cell area and coexpressed MHC-class II (Figure 3Ac).

### Defective *ex vivo* and *in vivo* migration of cutaneous DC in PI3K $\gamma$ -/- mice

The migratory ability of resident cutaneous DC was investigated in PI3K $\gamma$ -/- mice *ex vivo* and *in vivo*. When segments of dorsal ear skin were placed in culture, the number of MHC-class II<sup>+</sup> DC emigrating spontaneously into the culture medium, over a period of 2 days, was decreased in PI3K $\gamma$ -/- mice compared to WT animals (73.1%). In the presence of TNF or CCL21 in the incubation medium, a significant increase in the number of emigrant DC was observed in WT animals (178 and 236%, respectively;  $n = 10$ ). On the contrary, these two cytokines did not stimulate the egression of DC in PI3K $\gamma$ -/- mice (Figure 4A). To further evaluate the role of a PI3K $\gamma$  in TNF-induced DC migration *ex vivo*, experiments were performed in the presence of Wortmannin, a nonspecific inhibitor of PI3K isoforms, and *B. pertussis* toxin, an inhibitor of Gi protein-coupled chemotactic receptors. Figure 4B shows that both the treatments completely abrogated DC egression in response to TNF. Although no information are currently available on the effect of these two inhibitors on DC differentiation and maturation, *in vivo*, these results strongly suggest that the effect of TNF on DC migration is mediated by the secondary induction of chemotactic agonists.

Cutaneous DC migration was also evaluated after contact sensitization (Macatonia *et al*, 1987; Kripke *et al*, 1990). In this experimental model, FITC was applied to the skin of WT and PI3K $\gamma$ -/- mice and the number of FITC/CD11c double-positive cells recovered from the draining lymph nodes was evaluated by FACS analysis. Figure 4C shows that the appearance of CD11c<sup>+</sup>/FITC<sup>+</sup> in PI3K $\gamma$ -/- mice was strongly delayed and reduced (84.4% inhibition at 24 h) compared with WT mice ( $P < 0.001$ ). Reduced DC migration to lymph nodes was associated with a diminished increase in the total cellularity of the inguinal lymph nodes that increased 1.3-fold in PI3K $\gamma$ -/- mice following skin painting compared to the 2.0-fold increase observed in the WT mice (Figure 4D). It should be noted that under resting, unstimulated conditions, PI3K $\gamma$ -/- mice show a significant reduction in lymph node cellularity (Figure 4D). Histological analysis revealed that the few DC that were able to reach the draining lymph nodes in PI3K $\gamma$ -/- mice correctly localized to the T-cell-rich area (Figure 3Ae). In order to characterize the relative contribution of LC and dermal DC in the emigrated FITC<sup>+</sup> population, lymph node (LN) sections were stained for Langerin (Stoitzner *et al*, 2003) and double-positive cells (FITC<sup>+</sup>/Langerin<sup>+</sup>) were enumerated in WT and PI3K $\gamma$ -/- mice (Figure 3Af). Although the number of FITC<sup>+</sup> cells was greatly reduced in PI3K $\gamma$ -/- compared to WT mice (Figure 4C), the percentage of double-positive cells in the two experimental groups was similar (44 versus 50% at 24 h, and 71 versus 63% at 48 h, respectively). As expected, Langerin was not expressed by CFSE-labelled DC that migrated from the footpad to the draining lymph node (Figure 3Ad).

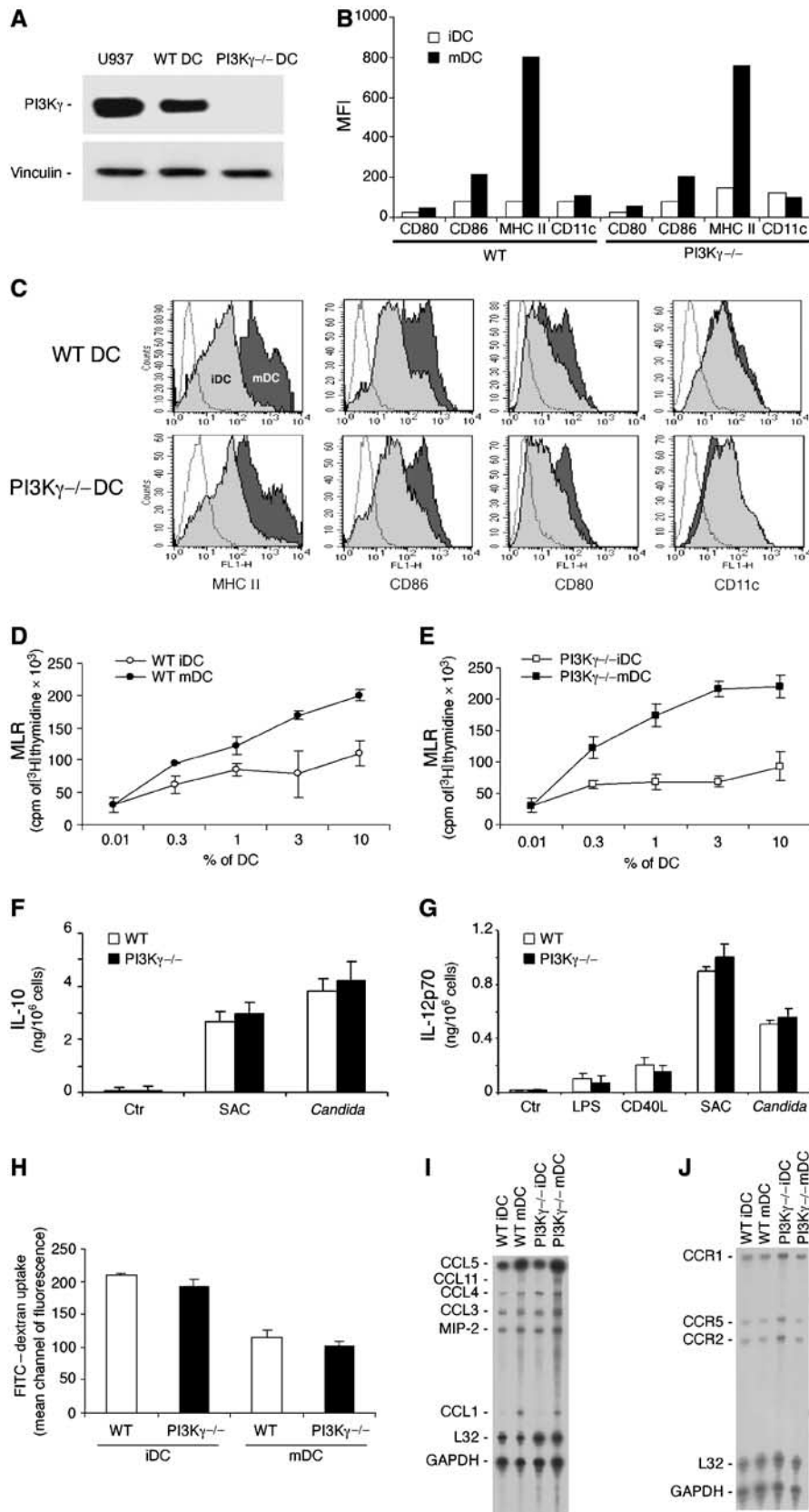


**Figure 1** Characterization of BM CD34-derived DC from WT and PI3K $\gamma$ <sup>-/-</sup> mice. Immature DC (iDC) and mature (20 ng/ml TNF- $\alpha$  for 24 h) DC (mDC) were generated from CD34<sup>+</sup> BM precursor cells *in vitro*. (A) Western blot analysis; (B, C) FACS analysis of the membrane phenotype; (D, E) MLR using DC from WT and PI3K $\gamma$ <sup>-/-</sup> mice; (F, G) cytokine determination in culture supernatants (24 h): CD40L (DC:J558, 4:1), LPS (100 mg/ml), SAC (1/100) *Candida albicans* (100  $\mu$ g/ml); (H) FITC-dextran uptake; (I, J) RPA analysis of chemokine and chemokine receptor expression. Each experiment is representative of 3–5 independent DC cultures.

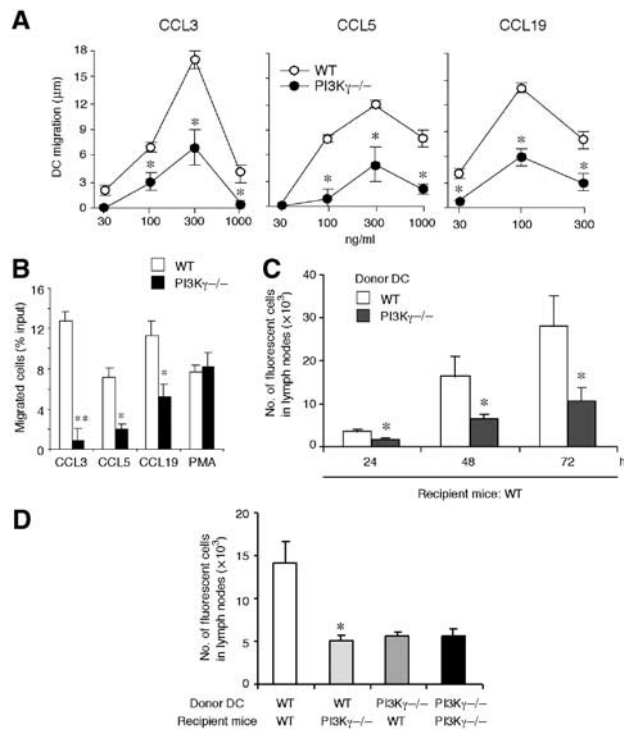


**Figure 2** Defective *in vitro* and *in vivo* migration of CD34-derived DC from PI3K $\gamma$ <sup>-/-</sup> mice. (A) Migration of iDC (to CCL3, CCL5) and TNF-mDC (to CCL19) was evaluated by the leading-front techniques, using nitrocellulose filters. The results are reported after subtraction of basal migration (against medium; 4±2 and 3±2 μm for WT and PI3K $\gamma$ <sup>-/-</sup> DC, respectively). (B) Migration of iDC and mDC was evaluated by Transwell insert. The results are at the net of basal migration: 5±2 and 3±2% for WT and PI3K $\gamma$ <sup>-/-</sup>, respectively. (C) TNF-mDC from WT and PI3K $\gamma$ <sup>-/-</sup> mice were labelled with the vital dye CFSE and injected subcutaneously in the hind leg footpad of WT mice. Popliteal lymph nodes were recovered 24, 48 and 72 h later and the cell suspension was evaluated by flow cytometry. (D) WT and PI3K $\gamma$ <sup>-/-</sup> TNF-mDC were injected either in WT or PI3K $\gamma$ <sup>-/-</sup> mice and recovered after 48 h. In panels C and D, results are expressed as the number of fluorescent cells recovered from the draining lymph nodes. Each experiment is representative of four experiments (\*\**P*<0.01, \**P*<0.05 versus respective WT control group).

### Distribution of DC subsets under steady-state conditions

The results discussed so far indicate that PI3K $\gamma$ <sup>-/-</sup> DC have defective migration *in vitro*, *ex vivo* and *in vivo*. We therefore examined in more detail the occurrence and distribution of DC in the skin and lymph nodes. Analysis of epidermal sheets from PI3K $\gamma$ <sup>-/-</sup> mice revealed that LC, evaluated as MHC-class II<sup>+</sup> cells, are reduced by ~45% in the skin of PI3K $\gamma$ <sup>-/-</sup> compared to WT mice (Figure 3Ba and b). In order to characterize both LC and dermal DC in the epidermis and dermis of the same section, skin vertical sections were obtained and stained for anti-MHC-class II molecules. The number of cells was evaluated and normalized with respect to the number of DAPI<sup>+</sup> basal keratinocytes present in the same fields; more than 200 keratinocytes were counted in each histological section (Bauer *et al*, 2001) (Figure 3Bc). Figure 3B shows, once again, that in the skin of PI3K $\gamma$ <sup>-/-</sup> mice (panel e) the number of LC was reduced compared to WT (panel d). After normalization with the number of keratinocytes, this reduction was quantified as equal to

50.0% (*n*=4; *P*<0.01). On the contrary, dermal DC were only partially reduced (37%; *n*=4), and this difference did not reach statistical significance (*P*<0.1).

DC subpopulations were further investigated in skin draining lymph nodes. Although the total number of leucocytes was reduced by 52% (*P*<0.01), the relative distribution of T and B cells was normal with only a partial increase (38%, *P*<0.02) of Mac-1<sup>+</sup> cells (Figure 4D and data not shown). Figure 5 shows that CD11c<sup>+</sup>/CD8 $\alpha$ <sup>+</sup> DC and plasmacytoid DC (CD11c<sup>+</sup>/CD11b<sup>-</sup>/B220<sup>+</sup>/Gr-1<sup>+</sup>) were present in a similar frequency in the inguinal lymph nodes obtained from WT and PI3K $\gamma$ <sup>-/-</sup> mice. On the contrary, the presence of CD11c<sup>+</sup>/CD8 $\alpha$ <sup>-</sup> DC was strongly reduced (62.7% reduction; *n*=7; *P*<0.01) in PI3K $\gamma$ <sup>-/-</sup> mice with respect to WT animals. It is interesting to note that a normal number of the latter subset was found in the spleen (3.8±0.3 and 3.6±0.4% in WT and PI3K $\gamma$ <sup>-/-</sup>, respectively), suggesting that PI3K $\gamma$ <sup>-/-</sup> mice do not have a defect in the differentiation of this DC subset from progenitor cells.

### Defective contact hypersensitivity in PI3K $\gamma$ <sup>-/-</sup> mice

Based on the results discussed above, it was of interest to test PI3K $\gamma$ <sup>-/-</sup> mice for their ability to mount specific immune responses. Accordingly, PI3K $\gamma$ <sup>-/-</sup> mice were used in a contact hypersensitivity (CHS) model performed with FITC and 2,4-dinitro-fluorobenzene (DNFB) as antigens. Figure 6A (left panel) shows the response of WT and PI3K $\gamma$ <sup>-/-</sup> mice sensitized on day 0 and locally challenged 5 days later with FITC. CHS reaction in WT mice was maximal at 18–24 h, and gradually decreased thereafter. PI3K $\gamma$ <sup>-/-</sup> mice demonstrated a reduced degree of ear swelling compared with that of WT animals (*P*<0.01 at 18 and 24 h). Similar results were observed using DNFB (Figure 6A, right panel), and using a model of delayed hypersensitivity reaction and sheep red blood cells as the antigen (not shown). Histological examination was performed to characterize CHS reaction in PI3K $\gamma$ <sup>-/-</sup> mice. Multiple subserial sections of ears skin were analysed upon CHS induction with DNFB (24 h). On haematoxylin/eosin staining, no histological abnormalities were observed in unstimulated control PI3K $\gamma$ <sup>-/-</sup> versus WT mice (Figure 6Ba and data not shown). Upon CHS induction, only scattered leucocytes were observed in the dermis of PI3K $\gamma$ <sup>-/-</sup> mouse (Figure 6Bb); in contrast, in WT animals, diffuse dermal oedema, vascular dilatation and an inflammatory infiltrate were evident (Figure 6Bc). The latter was variable in density and was predominantly composed of neutrophils, scattered eosinophils (Figure 6Bd) and mononuclear cells, which formed clusters and corresponded to macrophage/DC in terms of morphology, reactivity for MHC-class II molecules and the lack of CD3 expression (Figure 6Be–g and data not shown).

### Defective CHS response in PI3K $\gamma$ <sup>-/-</sup> mice following *in vivo* inoculation of antigen-loaded DC

In the light of the complex role of PI3K $\gamma$  in DC and lymphocyte biology (Sasaki *et al*, 2000; Rodriguez-Borlado *et al*, 2003), it was important to elucidate the role of DC in the defect of CHS response reported above (Figure 6). To this goal, bone marrow (BM)-derived mature DC from WT and PI3K $\gamma$ <sup>-/-</sup> mice, after *in vitro* loading with antigen (2,4-dinitrobenzene sulphonic acid (DNBS)), were inoculated into naive WT recipient mice. Figure 7A shows that mice

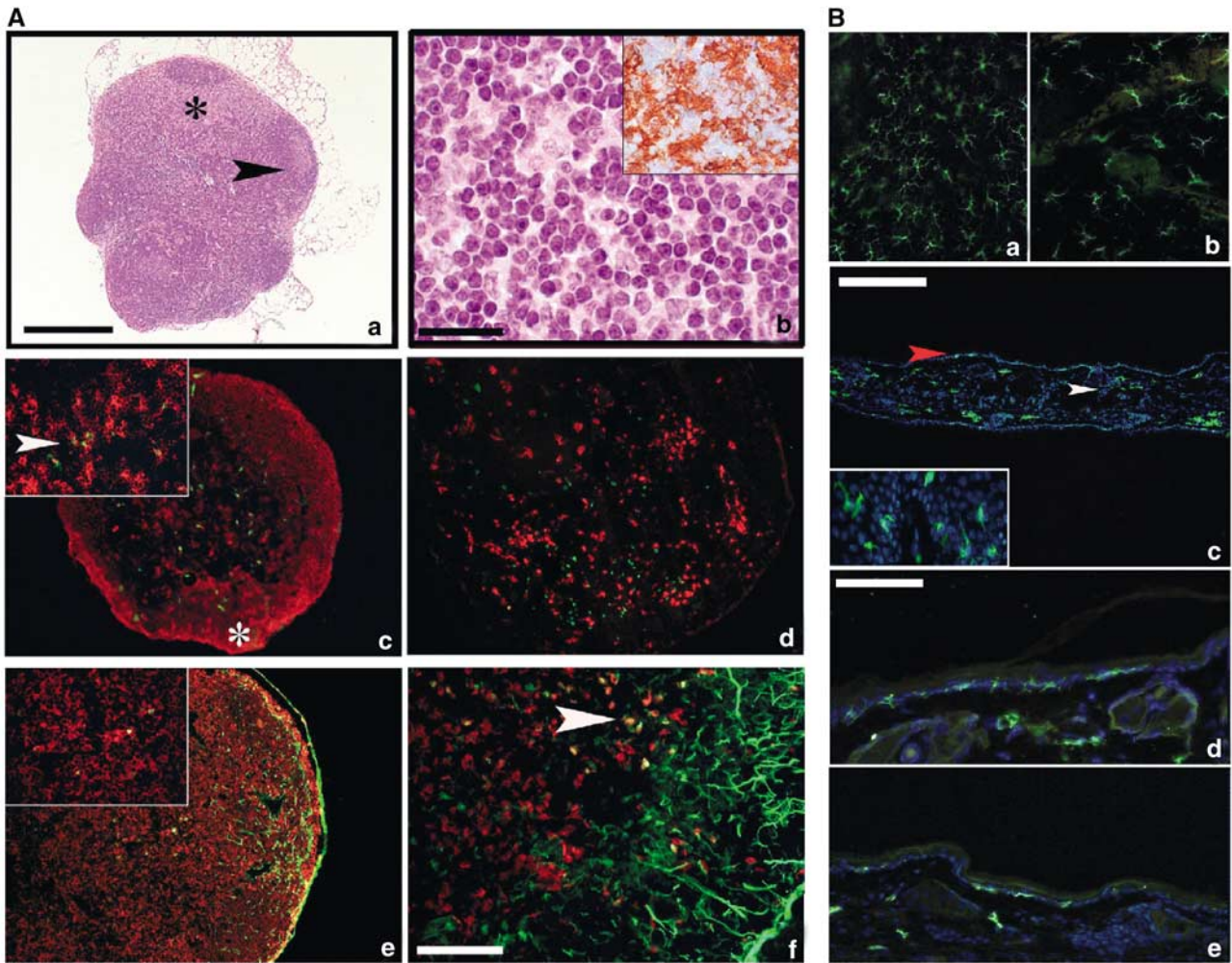


**Figure 3** Morphology and DC distribution in PI3K $\gamma$ <sup>-/-</sup> lymph nodes and skin sections under steady-state and inflammatory conditions. (A) Haematoxylin/eosin staining of a lymph node section from PI3K $\gamma$ <sup>-/-</sup> mice (a) displays normal architecture including cortex, with full-blown germinal centre (black arrow), and an expanded paracortex (black asterisk) populated by cells with dendritic morphology (b) with strong expression of MHC-class II (inset in b). Sections from a popliteal lymph node obtained after injection of CFSE-labelled DC immunostained for MHC-class II (red in c). A low-power field reveals two cortical nodules of MHC-class II<sup>+</sup> cells representing B-cell follicles (white asterisk) and sparse MHC-class II<sup>+</sup> cells with DC morphology, some of which are labelled by CFSE green fluorescent material in their cytoplasm (inset in c, arrow). Langerin-positive cells populate the subcortical area but do not contain CFSE green fluorescent material (d). Sections from an inguinal lymph node obtained after FITC-based skin painting were counterstained with MHC-class II molecule (e) and Langerin (f). The marginal sinus is filled with green fluorescent material and scattered cells in the paracortex contain green dots in their cytoplasm; these cells express MHC-class II<sup>+</sup> (inset in e) and some of them also Langerin (f; yellow cells, see arrows). Magnification  $\times 40$  (a, c, d and e; scale bar in a: 500  $\mu$ m),  $\times 100$  (f; scale bar: 200  $\mu$ m),  $\times 200$  (b; scale bar: 100  $\mu$ m) and  $\times 400$  (insets). Anti-MHC-class II-positive cells were detected by the immunoperoxidase technique (inset in b) and immunofluorescence (c, e (red staining)); Langerin was detected by immunofluorescence (d, f (red staining)). (B) (a, b) Two representative examples of epidermal sheets respectively from WT and PI3K $\gamma$ <sup>-/-</sup> animals, immunostained for MHC-class II molecule. MHC-class II<sup>+</sup> cells show a typical stellate morphology and regular distribution; an evident reduction in number is observed in PI3K $\gamma$ <sup>-/-</sup> epidermis (b). A low-power field from an entire representative section obtained from WT mice ears (c) lined by two thin layers of epidermis. MHC-class II<sup>+</sup> green cells are present in the epidermis (red arrow) as well as in the superficial dermis (white arrow) corresponding respectively to LC and to dermal DC. MHC-class II<sup>+</sup> LC display fine and long dendrites and multiple interactions with the surrounding keratinocytes (inset). A representative high-power field from WT skin section (d) shows numerous MHC-class II<sup>+</sup> LC and dermal DC homogeneously distributed. In PI3K $\gamma$ <sup>-/-</sup> (e), a reduced population of MHC-class II<sup>+</sup> LC is observed. Immunofluorescence analyses were performed with FITC-conjugated anti-MHC-class II (green) and nuclei were counterstained with DAPI. Magnification  $\times 40$  (c; scale bar: 500  $\mu$ m),  $\times 200$  (a, b, d, e; scale bar in d: 100  $\mu$ m) and  $\times 400$  (inset in c).

that had received DNBS-loaded WT DC could respond to a subsequent skin challenge with antigen (DNFB). This response was specific, since it was not observed when the challenge was performed with a different antigen, 4-ethoxy-methylene-2-phenyl-2-oxazoline-5-one (oxazolone, OXA) (Figure 7B). DC that were not loaded with the antigen failed to sensitize mice for a DNFB-specific CHS (data not shown). Conversely, WT mice injected with DNBS-loaded PI3K $\gamma$ <sup>-/-</sup> DC were unable to develop a normal CHS response to a

subsequent DNFB challenge at all the time points investigated ( $P < 0.001$ ).

## Discussion

This study shows that DC generated from CD34<sup>+</sup> BM precursors obtained from PI3K $\gamma$ <sup>-/-</sup> mice have a reduced ability to migrate in response to chemokines in chemotaxis assays *in vitro*, *ex vivo* and *in vivo*. *In vivo*, skin DC displayed an



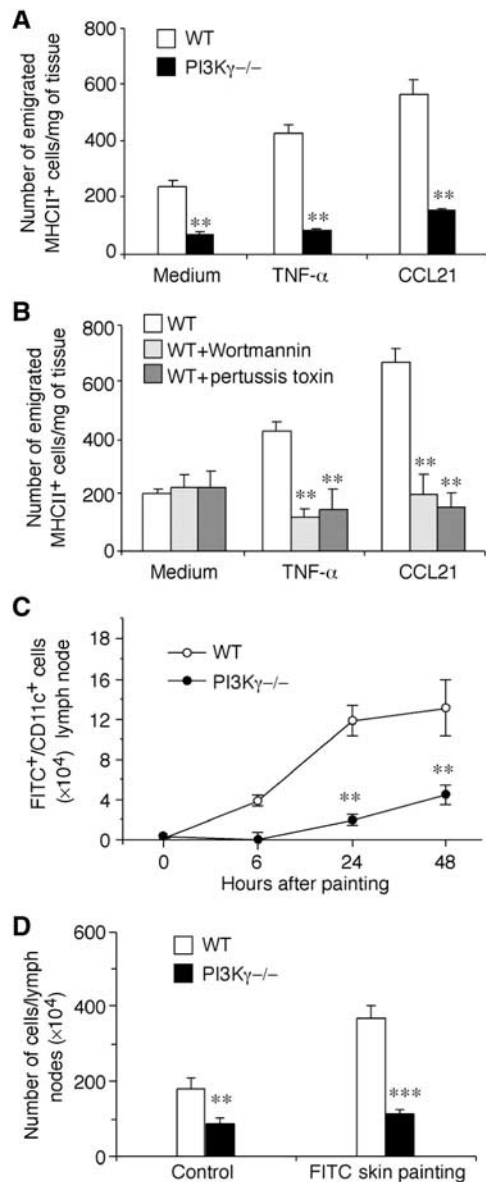


**Figure 4** Impaired migration of cutaneous DC in PI3K $\gamma$ <sup>-/-</sup> mice. (A) Number of MHC II<sup>+</sup> DC/skin explant, emigrated into the culture medium after 48 h (medium, 20 ng/ml TNF- $\alpha$ , 100 ng/ml CCL21). (B) Number of WT MHC II<sup>+</sup> DC (for each explant) emigrated in the presence of Wortmannin (30 nM) or pertussis toxin (600 ng/ml). (C) Number of FITC<sup>+</sup>/CD11c<sup>+</sup> DC in lymph nodes following FITC skin painting. The results are the mean  $\pm$  s.e.m. of one representative experiment (eight mice per group) out of the three performed. (D) Total lymph node cellularity was evaluated in control mice and after FITC skin painting. The results are the mean  $\pm$  s.e.m. of one representative experiment (eight mice per group) out of the four performed (\*\* $P$ <0.01, \*\*\* $P$ <0.001).

impaired ability to travel to the draining lymph nodes following local antigen administration. The number of CD11c<sup>+</sup>/FITC<sup>+</sup> DC recovered from inguinal lymph nodes was dramatically reduced (85%) in PI3K $\gamma$ <sup>-/-</sup> mice when compared to WT animals. This reduction far exceeded the decrease in the number of resident LC (50%) and dermal DC (37%) observed in PI3K $\gamma$ <sup>-/-</sup> mice. Nevertheless, once they reached the lymph node, PI3K $\gamma$ <sup>-/-</sup> DC localized as normal to the T-cell paracortical areas. The LC/dermal DC ratio in the FITC<sup>+</sup>

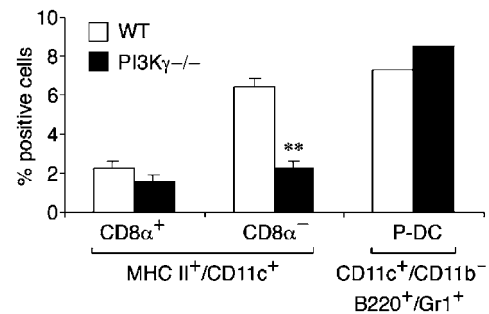


**Figure 5** Selective reduction of lymph node CD8 $\alpha$ <sup>-</sup> DC in PI3K $\gamma$ <sup>-/-</sup> mice. DC subsets were characterized in peripheral lymph nodes from WT and PI3K $\gamma$ <sup>-/-</sup> mice. MHC-class II<sup>+</sup> DC were gated and stained for CD11c and CD8 $\alpha$ . Plasmacytoid DC (P-DC) were identified as B220<sup>+</sup>/Gr-1<sup>+</sup> cells within a CD11c<sup>+</sup>/CD11b<sup>-</sup> population. The results are expressed as the percentage of MHC-class II<sup>+</sup> positive cells (\*\* $P$ <0.01;  $n$ =7). The results for P-DC are the average of two experiments.

population that migrated to lymph nodes was similar in WT and PI3K $\gamma$ <sup>-/-</sup> mice, indicating that the migration of both cell populations was similarly affected under stimulated conditions. Lymph nodes from PI3K $\gamma$ <sup>-/-</sup> mice have a reduced total cellularity (52%) when compared to WT mice. This defect could result in a reduced ability of lymph nodes to recruit DC, as previously suggested for rag2<sup>-/-</sup> mice (Shreedhar *et al*, 1999). With regard to this, WT DC showed a decreased ability to home to lymph nodes of PI3K $\gamma$ <sup>-/-</sup> mice. Therefore, it is possible that the defect in the migration of PI3K $\gamma$ <sup>-/-</sup> DC observed *in vitro* is further enhanced *in vivo* in PI3K $\gamma$ <sup>-/-</sup> mice. However, no additional defect in the migration of PI3K $\gamma$ <sup>-/-</sup> DC to lymph node was observed in PI3K $\gamma$ <sup>-/-</sup> versus WT mice.

The reduced migration of antigen-loaded DC from the skin to lymph nodes was associated with a reduced CHS response to both FITC and DNFB. This finding complements a previous study that has demonstrated that PI3K $\gamma$  is required to generate an effective T-cell response following lymphocytic choriomeningitis virus challenge and hapten immunization (Sasaki *et al*, 2000). These previous results, however, did not address the relative role of DC and T cells in the impaired antiviral cell-mediated immune response. To address the role of DC in defective CHS, DC, generated *in vitro* from both PI3K $\gamma$ <sup>-/-</sup> and WT BM precursors, were loaded with antigen and used in adoptive transfer experiments. When WT mice were injected with PI3K $\gamma$ <sup>-/-</sup> DC, less than 50% CHS response could be detected following subsequent challenge with DNFB. Since PI3K $\gamma$ <sup>-/-</sup> DC had the same ability to take up antigen *in vitro* and to induce T-cell proliferation, it is logical to assume that the defective CHS response observed in this experimental model is related to the impaired ability of antigen-loaded DC to travel *in vivo*. Therefore, it is likely that the defect of CHS response observed in PI3K $\gamma$ <sup>-/-</sup> mice is the combined result of a defective DC sensitization phase and an impaired subsequent generation of T-cell effector response.

Several studies have clearly indicated that DC migration to lymph nodes under inflammatory conditions is dependent on the expression of appropriate chemotactic factors and adhesion molecules (Campbell and Butcher, 2000; Weiss *et al*, 2001; Cavanagh and Von Andrian, 2002; Luster, 2002; McColl,

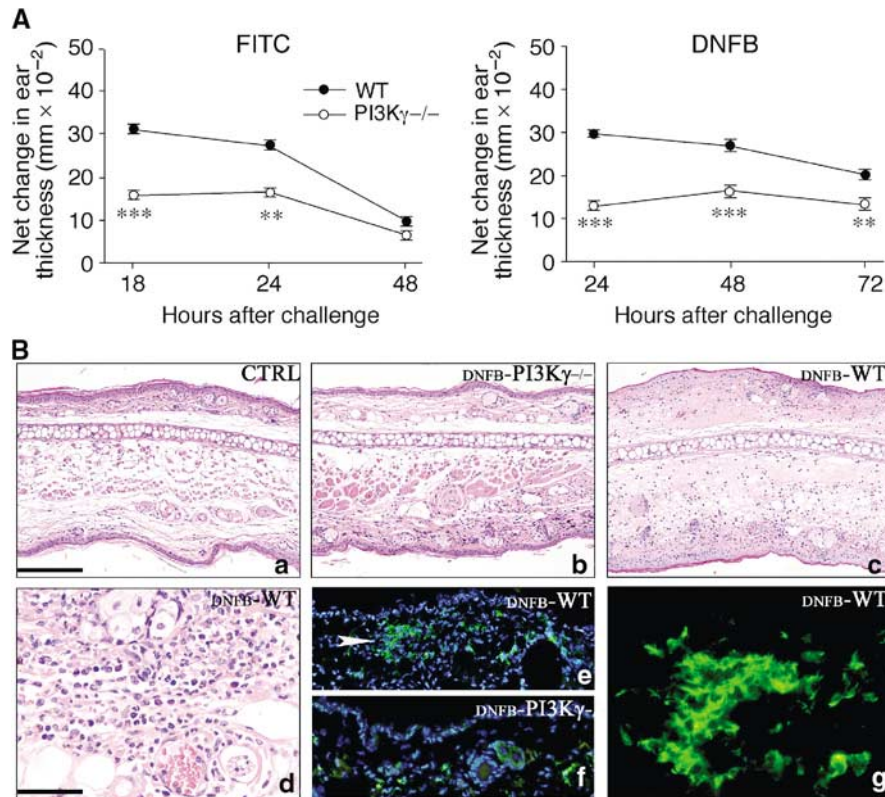


**Figure 6** Defective CHS in PI3K $\gamma$ <sup>-/-</sup> mice. **(A)** WT and PI3K $\gamma$ <sup>-/-</sup> were sensitized with FITC (left panel) or DNFB (right panel) on their shaved abdominal skin on day 0. After 5 days, mice were challenged on the right ear. The left ear was painted with vehicle as control. Increases in ear swelling were measured at different time points and are presented as increased swelling at the net of contralateral ear value. Mean  $\pm$  s.d. for each group (eight mice) are presented (\*\* $P$  < 0.01; \*\*\* $P$  < 0.001 versus respective WT group, by ANOVA Tukey's multiple comparison test). Each experiment is representative of three experiments. **(B)** Skin sections are obtained from unstimulated control (CTRL) animals (a), and after CHS induction with DNFB (24 h after challenging) respectively from PI3K $\gamma$ <sup>-/-</sup> (DNFB-PI3K $\gamma$ <sup>-/-</sup>) (b, f) and WT (DNFB-WT) (c, d, e, g). Upon CHS induction, only scattered leucocytes infiltrate the dermis of PI3K $\gamma$ <sup>-/-</sup> (b); in contrast, in WT mice, a diffuse dermal oedema is observed in association with microvascular dilatation and dense inflammatory infiltrate; the latter predominantly includes granulocytes, with occasional eosinophils and mononuclear cells (c, d); immunofluorescence demonstrates that the mononuclear cells exhibit a dendritic morphology, form aggregates and express MHC-class II antigens (e, white arrow head and g). This DC population is scant in PI3K $\gamma$ <sup>-/-</sup> and is represented by scattered cells (f). Magnification  $\times$  100 (a–c, e, f; scale bar in a: 200  $\mu$ m) and  $\times$  400 (d, g; scale bar in d: 50  $\mu$ m).

2002; Kabashima *et al*, 2003). Mice lacking CCR7 and CXCR5 have altered lymph node architecture, and present reduced numbers of DC in secondary lymphoid organs (Forster *et al*, 1996; Förster *et al*, 1999). Similarly, *plt* mice, a spontaneous mutant strain deficient in the CCL19 gene (one of the CCR7 ligands) expressed in high endothelial venules, have a reduced number of DC in the T-cell zone of lymph nodes (Gunn *et al*, 1999). CCR7<sup>-/-</sup> and *plt* mice, as well as mice defective in  $\beta$ 2 integrin function (Xu *et al*, 2001), show a reduced migration of cutaneous DC in skin sensitization experiments. Therefore, the results reported in this study strongly support a role for PI3K $\gamma$  in DC migration *in vivo*.

Although it is conceivable that the same classes of molecules that regulate DC migration in inflammatory conditions also direct the migration of these cells under normal conditions, little is known about the mechanisms that regulate the homing of DC, or their precursors, in steady-state conditions (Cavanagh and Von Andrian, 2002; McColl, 2002). Mice lacking the inflammatory chemokine receptors CCR2 and CCR6, the bioactive lipid receptor EP4, and CCR7 have a normal density of skin LC (Förster *et al*, 1999; Sato *et al*, 2000; Varona *et al*, 2001; Kabashima *et al*, 2003). Similarly,

ICAM-1<sup>-/-</sup> mice do not have any defect in the number of skin LC (Xu *et al*, 2001). In contrast, this study shows that PI3K $\gamma$ <sup>-/-</sup> mice have about 50% reduction in the number of skin LC. It is to be noted that these mice only express a minor reduction in the number of dermal DC. Two reports have recently shown an independent regulation of these two subsets of skin DC. First, mice deficient for KARAP/DAP12 (ITAM-bearing dimer that associates with a variety of membrane receptors expressed by NK and myeloid cells) present an increased number of dermal DC but a normal distribution of skin LC (Tomasello *et al*, 2000). Second, we have recently shown that patients with LAD-1, an immunodeficiency due to the lack of expression of functional  $\beta$ 2 integrins, have a selective defect in the number of factor XIIIa<sup>+</sup> cells (Fiorini *et al*, 2002). Factor XIIIa is a marker for interstitial DC that are located in the dermis (Nestle *et al*, 1993). Thus, *in vivo* localization of dermal DC is apparently more dependent on  $\beta$ 2 integrins and less sensitive to the absence of PI3K $\gamma$ . Although this study does not formally exclude that PI3K $\gamma$ <sup>-/-</sup> mice may have alterations at the level of specific LC cell precursors, the data discussed here suggest that the use of different adhesion molecule–chemotactic receptor pairs by

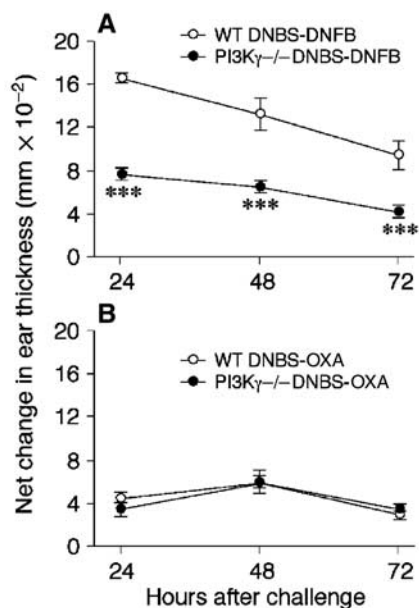


**Figure 7** Defective capacity of PI3K $\gamma$ <sup>-/-</sup> DC to elicit CHS. WT mice were immunized (on day -5) by subcutaneous injection of DNBS-loaded DC (10<sup>6</sup>/mouse) obtained from WT or PI3K $\gamma$ <sup>-/-</sup> mice. Mice were challenged 5 days later (day 0) by ear painting with DNFB (A) or oxazolone (OXA; B). The figures represent the values for ear swelling (mean  $\pm$  s.e.m.) of five mice per group, and are representative of three experiments (\*\*\*)  $P < 0.001$ .

LC versus dermal DC may account for a different homing of these two skin DC populations.

PI3K $\gamma$ <sup>-/-</sup> mice also presented a selective (62.7%) reduction of CD8 $\alpha$ <sup>-</sup> DC in skin draining lymph nodes. It is worth noting that the same DC subset is present in normal levels in the spleen. Whereas lymphocyte entry into lymph nodes and Peyer's patches involves transient rolling along the endothelial surface, firm adherence and transendothelial migration by a pertussis toxin-sensitive step, lymphocyte entry into the splenic parenchyma is pertussis toxin-insensitive and does not require active migration across an endothelial layer (Cyster and Goodnow, 1995). Thus, entry of leucocytes into the spleen is independent of chemotactic agonists, and it is likely that this difference is responsible for the normal numbers of CD8 $\alpha$ <sup>-</sup> cells in this lymphoid organ. Nevertheless, the finding of normal numbers of CD8 $\alpha$ <sup>-</sup> DC in the spleen argues against the possibility that PI3K $\gamma$ <sup>-/-</sup> mice have a defect in their differentiation from progenitor cells. The two other DC subsets investigated (i.e. CD8 $\alpha$ <sup>+</sup> and CD11b<sup>-</sup>/B220<sup>+</sup>/Gr-1<sup>+</sup>) were present in normal numbers in the lymph nodes of PI3K $\gamma$ <sup>-/-</sup> mice. It is known that DC subtypes migrate in response to different chemotactic agonists *in vitro*, and differ in their migratory patterns *in vivo* (Steinman, 1991; Henri *et al*, 2001; Penna *et al*, 2001). Although the reason for the selective reduction of CD8 $\alpha$ <sup>-</sup> DC in lymph nodes is not known, it seems reasonable to speculate that CD8 $\alpha$ <sup>-</sup> DC use a different pattern of molecules than CD8 $\alpha$ <sup>+</sup> and plasmacytoid DC for their *in vivo* migration, and that this process is more dependent on the expression of PI3K $\gamma$ .

In a recent study, it was reported that mice lacking the p85 $\alpha$  regulatory subunit of PI3K (class IA) have a normal distribution of DC subsets in the spleen (Fukao *et al*, 2002).

However, DC from these mice showed a dramatic increase in their ability to release IL-12p70, suggesting a negative regulatory function of PI3K in Th1 immune responses. In the present study, no difference in the production of IL-12 and IL-10 was observed in BM-derived DC from PI3K $\gamma$ <sup>-/-</sup> mice compared to WT DC. These results outline a complex scenario in which PI3K isoforms may regulate different biological functions of DC. In addition, these results also indicate that PI3K $\gamma$  is not involved in chemotactic agonist-mediated inhibition of IL-12 production (Braun *et al*, 2000; He *et al*, 2000).

Several studies have shown that lipid products of PI3K $\gamma$  play a role as 'compass' molecules by controlling the direction of cell migration and the intracellular localization of F-actin and signalling molecules at the leading edge (Rickert *et al*, 2000). This study extends these findings to DC, a leucocyte population that plays a pivotal role in the generation of specific immunity. DC from PI3K $\gamma$ <sup>-/-</sup> mice had a reduced ability to migrate in response to chemotactic factors both *in vitro* and *in vivo*. Most importantly, the results presented here show that the reduced ability of antigen-loaded DC to travel *in vivo* was associated with a reduced ability of PI3K $\gamma$ <sup>-/-</sup> mice to mount T-cell-mediated specific immune responses in different experimental systems. Therefore, these results indicate that PI3K $\gamma$  may represent a new valuable target to control inappropriate activation of specific immune responses.

## Materials and methods

### Cytokines

Human CCL3, CCL19 and murine CCL5 were from Peprotech Inc. (Rocky Hill, NJ). Mouse granulocyte-macrophage colony-stimulating factor (GM-CSF) was from Sandoz (Basel, Switzerland) and murine TNF- $\alpha$  was a kind gift from Dr P Vandenabeele (Gent University, Belgium). Human Flt3 ligand was a generous gift from Immunex (Seattle, WA). Cytokines were endotoxin free as assessed by Limulus amoebocyte assay (BioWhittaker Inc., Walkersville, MD).

### Flow cytometry

mAbs used were from BD-Pharmingen and included phycoerythrin (PE)-conjugated hamster anti-mouse CD11c (IgG1, clone HL3), APC-conjugated rat anti-mouse CD11b (IgG2b, clone M1/70), PerCP-Cy5.5-conjugated rat anti-mouse Gr-1 (IgG2b, clone RB6-8C5), FITC-conjugated rat anti-mouse CD45/B220 (IgG2a, clone RA3-6B2), APC-conjugated rat anti-mouse CD8 $\alpha$  (IgG2a, clone 53-6.7), FITC-conjugated rat anti-mouse MHC-class II (IgG2a, clone 2G9) and rat anti-mouse CD80 (IgG2a, clone 1G10). Rat anti-mouse CD86 was from ATCC (HB-253). Cells were analysed by FACScan.

### Dendritic cell culture

For the study, 8- to 12-week-old 129sv WT and 129sv PI3K $\gamma$ <sup>-/-</sup> male mice were used (Hirsch *et al*, 2000). CD34<sup>+</sup>-derived myeloid DC (DC) were generated and functionally characterized as previously described (Vecchi *et al*, 1999).

### Chemotaxis assay

Cell migration was evaluated either by using a 48-well chemotaxis chamber (Neuroprobe, Pleasanton, CA) with 150  $\mu$ m nitrocellulose filters (5  $\mu$ m pore size; Neuroprobe) or using Transwell inserts (Corning, Life Science). Chemotaxis was evaluated after 90 min incubation as the distance (in  $\mu$ m) migrated by the two leading cells (nitrocellulose filters) or the percentage of input cells migrated across the filter (Transwell assay) (Zigmond and Hirsch, 1973; Sozzani *et al*, 1995).



### **In vivo migration of murine DC**

WT and PI3K $\gamma$ -/- mature DC from a 9 days culture were labelled with 0.5  $\mu$ M of the vital dye 5-(and-6)-carboxyfluorescein diacetate succinimidyl ester, mixed isomer (5-(6)-CFDA, SE (CFSE), Molecular Probes Inc., Eugene, OR). A total of  $2 \times 10^6$  labelled cells were injected subcutaneously in the hind leg footpad. Popliteal lymph nodes were recovered 24, 48 and 72 h later, mechanically disaggregated and treated with collagenase A (1 mg/ml; Boehringer Mannheim, Indianapolis, IN) and DNase (0.4 mg/ml; Roche, Indianapolis, IN) mixture for 30 min; the enzymatically treated cell suspension was evaluated by FACScan (Becton Dickinson, San Jose, CA).

### **In vitro DC migration from mouse ear skin**

Murine ears were rinsed in 70% ethanol, air-dried and split in dorsal and ventral halves. Dorsal skin was placed split-side down in 1 ml of RPMI 1640 culture medium, 10% fetal calf serum (FCS), 2-mercaptoethanol (2-ME) and 1% fungizone. After 48 h, cells were collected, counted and the percentage of FITC/MHC-class II<sup>+</sup> cells was evaluated using a fluorescent microscope on cytospin preparations (Ortner *et al*, 1996).

### **FITC skin painting**

FITC (fluorescein isothiocyanate isomer I, Sigma, St Louis, MO) was dissolved in a 50:50 (vol/vol) acetone-dibutylphthalate (BDH) mixture just before application. Mice were painted on the shaved abdomen with 0.2 ml/5 mg/ml FITC. After 24 h, inguinal lymph nodes were disaggregated and treated with collagenase A/DNase mixture for 30 min. Cell suspensions were then stained with a PE-labelled anti-CD11c mAb and PE/FITC double-positive cells were analysed by FACScan (Macatonia *et al*, 1987).

### **Contact hypersensitivity**

DNFB (Sigma, St Louis), FITC and OXA (Sigma) were freshly prepared before CHS assays. DNBS (ICN Biomedical Inc., Aurora, OH) was used for *in vitro* pulsing of DC. For sensitization, mice were painted (day -5) on the shaved abdominal skin with 50  $\mu$ l of 0.5% DNFB in 4:1 acetone:olive oil (vol/vol) and 5  $\mu$ l on each footpad or 0.5% FITC in 1:1 acetone:dibutylphthalate (vol/vol) on the shaved abdomen. After 5 days (day 0), mice were challenged by the application of 10  $\mu$ l of DNFB (0.2%) or FITC (0.5%) on each side of the right ear, while the left ear received the vehicle alone. CHS response was determined by measuring the degree of ear swelling of the antigen-painted ear compared to that of the vehicle-treated contralateral ear at 24–72 h after challenge using a dial thickness gauge (Mitutoyo, Cardiff, UK). In some experiments, CHS response was evaluated after *in vivo* inoculation of antigen-loaded DC (Krasteva *et al*, 1998). BM-derived DC from WT and PI3K $\gamma$ -/- were resuspended in Hank's balanced salt solution without FCS containing DNBS (100  $\mu$ g/ml) and incubated at 37°C for 30 min. For sensitization (day -5),  $1 \times 10^6$  DNBS-BM-DC from WT and PI3K $\gamma$ -/- were injected subcutaneously into the flank of WT recipient mice, in 200  $\mu$ l of saline. After 5 days (day 0), mice were

challenged by the application of DNFB (0.2%) or OXA (1%), as control, on each side of the right ear. A group of mice injected with the same number of untreated DC served as a negative control.

### **Tissue staining and dendritic cell counts**

Epidermal sheets were prepared as previously described by incubation with ammonium thiocyanate (Angeli *et al*, 2001). Thin tissue sections from lymph nodes were obtained and stained with haematoxylin/eosin for morphological evaluation. For immunofluorescence analysis, lymph nodes and small fragments of mouse ears were embedded in Tissue Tec OCT, snap-frozen by immersion in liquid nitrogen-cooled isopentane and stored at -80°. Sections (3  $\mu$ m), fixed in acetone, were incubated with rat anti-mouse MHC-class II (0.5 mg/ml; dilution 1:50) and with anti-Langerin mAb (a kind gift of Dr G Trinchieri, Shering Plough, Dardilly, France). Lymph node sections were incubated with a biotinylated rabbit anti-rat IgG (mouse adsorbed; 0.5 mg/ml; Vector Lab., Burlingame, CA; dilution 1:200) and revealed with Texas red streptavidin or immunoperoxidase technique. For skin sections, an FITC-conjugated anti-rat IgG (1 mg/ml; Vector; dilution 1:50) was chosen. Nuclei were counterstained by the fluorochrome 4',6-diamidino-2-phenylindole (DAPI). Slides were analysed with a fluorescence microscope (Olympus BX60) and images were taken for quantification using a Nikon DN100 digital camera.

Quantitative analysis of epidermal and dermal DC expressing MHC-class II was performed by evaluating 40 high-power fields obtained from nonconsecutive ear sections. LC MHC-class II<sup>+</sup> numbers with stellar morphology were normalized for the number of basal keratinocytes. From the same area, the number of dermal DC, displaying either stellar or spindle-shaped morphology, was evaluated using Image Tool software (University of Texas, Science Centre, S Antonio) and expressed as number of cells/mm<sup>2</sup> of superficial dermis.

FITC- or CFSE-labelled DC were analysed in peripheral lymph nodes (inguinal and popliteal lymph nodes, respectively). Morphology and distribution of green autofluorescent cells as well as their colocalization with anti-MHC-class II cells were evaluated by fluorescence microscopy (Lyons, 2000).

### **Statistical analysis**

Experimental groups include at least five mice. All experiments were performed at least three times. Statistical significance was evaluated using the two-tailed Student's *t*-test.

## **Acknowledgements**

We thank Dr Silvana Festa for technical help and Dr Chris Scotton for critical reading of the manuscript. This work was supported by MIUR (Cofin), AIRC (Associazione Italiana per la Ricerca sul Cancro), by Association for International Cancer Research (grant no. 04-223) and by European Union Fifth Framework Programme QLGI-2001-02171 and QLK3-2001-01010.

## **References**

Allavena P, Sica A, Vecchi A, Locati M, Sozzani S, Mantovani A (2000) The chemokine receptor switch paradigm and dendritic cell migration: its significance in tumor tissues. *Immunol Rev* **177**: 141–149

Angeli V, Faveeuw C, Roye O, Fontaine J, Teissier E, Capron A, Wolowczuk I, Capron M, Trottein F (2001) Role of the parasite-derived prostaglandin D2 in the inhibition of epidermal Langerhans cell migration during schistosomiasis infection. *J Exp Med* **193**: 1135–1147

Baggiolini M (1998) Chemokines and leukocyte traffic. *Nature* **392**: 565–568

Banchereau J, Briere F, Caux C, Davoust J, Lebecque S, Liu YJ, Pulendran B, Palucka K (2000) Immunobiology of dendritic cells. *Annu Rev Immunol* **18**: 767–811

Banchereau J, Steinman RM (1998) Dendritic cells and the control of immunity. *Nature* **392**: 245–252

Bauer J, Bahmer FA, Worl J, Neuhuber W, Schuler G, Fartasch M (2001) A strikingly constant ratio exists between Langerhans cells and other epidermal cells in human skin. A stereologic study

using the optical disector method and the confocal laser scanning microscope. *J Invest Dermatol* **116**: 313–318

Braun MC, Lahey E, Kelsall BL (2000) Selective suppression of IL-12 production by chemoattractants. *J Immunol* **164**: 3009–3017

Brock C, Schaefer M, Reusch HP, Czupalla C, Michalke M, Spicher K, Schultz G, Nurnberg B (2003) Roles of G beta gamma in membrane recruitment and activation of p110 gamma/p101 phosphoinositide 3-kinase gamma. *J Cell Biol* **160**: 89–99

Campbell JJ, Butcher EC (2000) Chemokines in tissue-specific and microenvironment-specific lymphocyte homing. *Curr Opin Immunol* **12**: 336–341

Cavanagh LL, Von Andrian UH (2002) Travellers in many guises: the origins and destinations of dendritic cells. *Immunol Cell Biol* **80**: 448–462

Cella M, Sallusto F, Lanzavecchia A (1997) Origin, maturation and antigen presenting function of dendritic cells. *Curr Opin Immunol* **9**: 10–16

Charbonnier AS, Kohrgruber N, Kriehuber E, Stingl G, Rot A, Maurer D (1999) Macrophage inflammatory protein 3alpha is

- involved in the constitutive trafficking of epidermal Langerhans cells. *J Exp Med* **190**: 1755–1768
- Cyster JG (1999) Chemokines and the homing of dendritic cells to the T cell areas of lymphoid organs. *J Exp Med* **189**: 447–450
- Cyster JG, Goodnow CC (1995) Pertussis toxin inhibits migration of B and T lymphocytes into splenic white pulp cords. *J Exp Med* **182**: 581–586
- Fiorini M, Vermi W, Facchetti F, Moratto D, Alessandri G, Notarangelo L, Caruso A, Grigolato P, Ugazio AG, Notarangelo LD, Badolato R (2002) Defective migration of monocyte-derived dendritic cells in LAD-1 immunodeficiency. *J Leukoc Biol* **72**: 650–656
- Forster R, Mattis AE, Kremmer E, Wolf E, Brem G, Lipp M (1996) A putative chemokine receptor, BLR1, directs B cell migration to defined lymphoid organs and specific anatomic compartments of the spleen. *Cell* **87**: 1037–1047
- Förster R, Schubel A, Breitfeld D, Kremmer E, Renner-Müller I, Wolf E, Lipp M (1999) CCR7 coordinates the primary immune response by establishing functional microenvironments in secondary lymphoid organs. *Cell* **99**: 23–33
- Fukao T, Yamada T, Tanabe M, Terauchi Y, Ota T, Takayama T, Asano T, Takeuchi T, Kadowaki T, Hata Ji J, Koyasu S (2002) Selective loss of gastrointestinal mast cells and impaired immunity in PI3K-deficient mice. *Nat Immunol* **3**: 295–304
- Gunn MD, Kyuwu S, Tam C, Kakiuchi T, Matsuzawa A, Williams LT, Nakano H (1999) Mice lacking expression of secondary lymphoid organ chemokine have defects in lymphocyte homing and dendritic cell localization. *J Exp Med* **189**: 451–460
- He J, Gurunathan S, Iwasaki A, Ash-Shaheed B, Kelsall BL (2000) Primary role for Gi protein signaling in the regulation of interleukin 12 production and the induction of T helper cell type 1 responses. *J Exp Med* **191**: 1605–1610
- Henri S, Vremec D, Kamath A, Waithman J, Williams S, Benoist C, Burnham K, Saeland S, Handman E, Shortman K (2001) The dendritic cell populations of mouse lymph nodes. *J Immunol* **167**: 741–748
- Hirsch E, Katanaev VL, Garlanda C, Azzolino O, Pirola L, Silengo L, Sozzani S, Mantovani A, Altruda F, Wymann MP (2000) Central role for G protein-coupled phosphoinositide 3-kinase gamma in inflammation [see comments]. *Science* **287**: 1049–1053
- Homey B, Dieu-Nosjean MC, Wiesenborn A, Massacrier C, Pin JJ, Oldham E, Catron D, Buchanan ME, Muller A, deWaal Malefyt R, Deng G, Orozco R, Ruzicka T, Lehmann P, Lebecque S, Caux C, Zlotnik A (2000) Up-regulation of macrophage inflammatory protein-3 alpha/CCL20 and CC chemokine receptor 6 in psoriasis. *J Immunol* **164**: 6621–6632
- Kabashima K, Sakata D, Nagamachi M, Miyachi Y, Inaba K, Narumiya S (2003) Prostaglandin E2-EP4 signaling initiates skin immune responses by promoting migration and maturation of Langerhans cells. *Nat Med* **9**: 744–749
- Krasteva M, Kehren J, Horand F, Akiba H, Choquet G, Ducluzeau MT, Tedone R, Garrigue JL, Kaiserlian D, Nicolas JF (1998) Dual role of dendritic cells in the induction and down-regulation of antigen-specific cutaneous inflammation. *J Immunol* **160**: 1181–1190
- Kripke ML, Munn CG, Jeevan A, Tang JM, Bucana C (1990) Evidence that cutaneous antigen-presenting cells migrate to regional lymph nodes during contact sensitization. *J Immunol* **145**: 2833–2838
- Laffargue M, Calvez R, Finan P, Trifilieff A, Barbier M, Altruda F, Hirsch E, Wymann MP (2002) Phosphoinositide 3-kinase gamma is an essential amplifier of mast cell function. *Immunity* **16**: 441–451
- Li Z, Jiang H, Xie W, Zhang Z, Smrcka AV, Wu D (2000) Roles of PLC-beta2 and -beta3 and PI3Kgamma in chemoattractant-mediated signal transduction. *Science* **287**: 1046–1049
- Luster AD (2002) The role of chemokines in linking innate and adaptive immunity. *Curr Opin Immunol* **14**: 129–135
- Lyons AB (2000) Analysing cell division *in vivo* and *in vitro* using flow cytometric measurement of CFSE dye dilution. *J Immunol Methods* **243**: 147–154
- Macatonia SE, Knight SC, Edwards AJ, Griffiths S, Fryer P (1987) Localization of antigen on lymph node dendritic cells after exposure to the contact sensitizer fluorescein isothiocyanate. Functional and morphological studies. *J Exp Med* **166**: 1654–1667
- McColl SR (2002) Chemokines and dendritic cells: a crucial alliance. *Immunol Cell Biol* **80**: 489–496
- Nestle FO, Zheng XG, Thompson CB, Turka LA, Nickoloff BJ (1993) Characterization of dermal dendritic cells obtained from normal human skin reveals phenotypic and functionally distinctive subsets. *J Immunol* **151**: 6535–6545
- Ngo VN, Tang HL, Cyster JG (1998) Epstein-Barr virus-induced molecule 1 ligand chemokine is expressed by dendritic cells in lymphoid tissues and strongly attracts naive T cells and activated B cells. *J Exp Med* **188**: 181–191
- Ortner U, Inaba K, Koch F, Heine M, Miwa M, Schuler G, Romani N (1996) An improved isolation method for murine migratory cutaneous dendritic cells. *J Immunol Methods* **193**: 71–79
- Penna G, Sozzani S, Adorini L (2001) Cutting edge: selective usage of chemokine receptors by plasmacytoid dendritic cells. *J Immunol* **167**: 1862–1866
- Rickert P, Weiner OD, Wang F, Bourne HR, Servant G (2000) Leukocytes navigate by compass: roles of PI3Kgamma and its lipid products. *Trends Cell Biol* **10**: 466–473
- Rodríguez-Borlado L, Barber DF, Hernandez C, Rodríguez-Marcos MA, Sanchez A, Hirsch E, Wymann M, Martinez AC, Carrera AC (2003) Phosphatidylinositol 3-kinase regulates the CD4/CD8T cell differentiation ratio. *J Immunol* **170**: 4475–4482
- Sallusto F, Lanzavecchia A (1999) Mobilizing dendritic cells for tolerance, priming, and chronic inflammation. *J Exp Med* **189**: 611–614
- Sasaki T, Irie-Sasaki J, Jones RG, Oliveira-dos-Santos AJ, Stanford WL, Bolon B, Wakeham A, Itie A, Bouchard D, Koziarzdzki I, Joza N, Mak TW, Ohashi PS, Suzuki A, Penninger JM (2000) Function of PI3Kgamma in thymocyte development, T cell activation, and neutrophil migration. *Science* **287**: 1040–1046
- Sasaki T, Suzuki A, Sasaki J, Penninger JM (2002) Phosphoinositide 3-kinases in immunity: lessons from knockout mice. *J Biochem (Tokyo)* **131**: 495–501
- Sato N, Ahuja SK, Quinones M, Kostecki V, Reddick RL, Melby PC, Kuziel WA, Ahuja SS (2000) CC chemokine receptor (CCR)2 is required for Langerhans cell migration and localization of T helper cell type 1 (Th1)-inducing dendritic cells. Absence of CCR2 shifts the Leishmania major-resistant phenotype to a susceptible state dominated by Th2 cytokines, B cell outgrowth, and sustained neutrophilic inflammation. *J Exp Med* **192**: 205–218
- Shreedhar V, Moodycliffe AM, Ullrich SE, Bucana C, Kripke ML, Flores-Romo L (1999) Dendritic cells require T cells for functional maturation *in vivo*. *Immunity* **11**: 625–636
- Sozzani S, Allavena P, D'Amico G, Luini W, Bianchi G, Kataura M, Imai T, Yoshie O, Bonecchi R, Mantovani A (1998) Differential regulation of chemokine receptors during dendritic cell maturation: a model for their trafficking properties. *J Immunol* **161**: 1083–1086
- Sozzani S, Sallusto F, Luini W, Zhou D, Piemonti L, Allavena P, Van Damme J, Valitutti S, Lanzavecchia A, Mantovani A (1995) Migration of dendritic cells in response to formyl peptides, C5a, and a distinct set of chemokines. *J Immunol* **155**: 3292–3295
- Steinman RM (1991) The dendritic cell system and its role in immunogenicity. *Annu Rev Immunol* **9**: 271–296
- Steinman RM, Hawiger D, Nussenzweig MC (2003) Tolerogenic dendritic cells. *Annu Rev Immunol* **21**: 685–711
- Stephens LR, Eguinoa A, Erdjument-Bromage H, Lui M, Cooke F, Coadwell J, Smrcka AS, Thelen M, Cadwallader K, Tempst P, Hawkins PT (1997) The G beta gamma sensitivity of a PI3K is dependent upon a tightly associated adaptor, p101. *Cell* **89**: 105–114
- Stoitzner P, Holzmann S, McLellan AD, Ivarsson L, Stossel H, Kapp M, Kammerer U, Douillard P, Kampgen E, Koch F, Saeland S, Romani N (2003) Visualization and characterization of migratory Langerhans cells in murine skin and lymph nodes by antibodies against Langerin/CD207. *J Invest Dermatol* **120**: 266–274
- Stoyanova S, Vanhaesebroeck B, Dhand R, Nürnberg B, Gierschik P, Seedorf K, Hsuan JJ, Waterfield MD, Wetzer R (1995) Cloning and characterization of a G protein-activated human phosphoinositide-3 kinase. *Science* **269**: 690–693
- Tomasello E, Desmouliens PO, Chemin K, Guia S, Cremer H, Ortaldo J, Love P, Kaiserlian D, Vivier E (2000) Combined natural killer cell and dendritic cell functional deficiency in KARAP/DAP12 loss-of-function mutant mice. *Immunity* **13**: 355–364

- Varona R, Villares R, Carramolino L, Goya I, Zaballos A, Gutierrez J, Torres M, Martinez AC, Marquez G (2001) CCR6-deficient mice have impaired leukocyte homeostasis and altered contact hypersensitivity and delayed-type hypersensitivity responses. *J Clin Invest* **107**: R37–R45
- Vecchi A, Massimiliano L, Ramponi S, Luini W, Bernasconi S, Bonecchi R, Allavena P, Parmentier M, Mantovani A, Sozzani S (1999) Differential responsiveness to constitutive versus inducible chemokines of immature and mature mouse dendritic cells. *J Leukoc Biol* **66**: 489–494
- Ward SG (2004) Do phosphoinositide 3-kinases direct lymphocyte navigation? *Trends Immunol* **25**: 67–74
- Weiss JM, Renkl AC, Maier CS, Kimmig M, Liaw L, Ahrens T, Kon S, Maeda M, Hotta H, Uede T, Simon JC (2001) Osteopontin is involved in the initiation of cutaneous contact hypersensitivity by inducing Langerhans and dendritic cell migration to lymph nodes. *J Exp Med* **194**: 1219–1229
- Willmann K, Legler DF, Loetscher M, Roos RS, Delgado MB, Clark-Lewis I, Baggiolini M, Moser B (1998) The chemokine SLC is expressed in T cell areas of lymph nodes and mucosal lymphoid tissues and attracts activated T cells via CCR7. *Eur J Immunol* **28**: 2025–2034
- Wymann MP, Sozzani S, Altruda F, Mantovani A, Hirsch E (2000) Lipids on the move: phosphoinositide 3-kinases in leukocyte function. *Immunol Today* **21**: 260–264
- Xu H, Guan H, Zu G, Bullard D, Hanson J, Slater M, Elmets CA (2001) The role of ICAM-1 molecule in the migration of Langerhans cells in the skin and regional lymph node. *Eur J Immunol* **31**: 3085–3093
- Zigmond SH, Hirsch JG (1973) Leukocyte locomotion and chemotaxis. New methods for evaluation, and demonstration of a cell-derived chemotactic factor. *J Exp Med* **137**: 387–410
- Zlotnik A, Yoshie O (2000) Chemokines: a new classification system and their role in immunity. *Immunity* **12**: 121–127